frontiers | Frontiers in Endocrinology

TYPE Original Research
PUBLISHED 02 September 2022
DOI 10.3389/fendo.2022.909207

OPEN ACCESS

EDITED BY
Undurti Narasimha Das,
UND Life Sciences LLC, United States

REVIEWED BY
Norbert Nass,
Städtische Klinikum Dessau, Germany
Dong Hyun Jo,
Seoul National University, South Korea

*CORRESPONDENCE
Jing Luo
luojing001@csu.edu.cn

SPECIALTY SECTION
This article was submitted to Diabetes: Molecular Mechanisms, a section of the journal Frontiers in Endocrinology

RECEIVED 31 March 2022
ACCEPTED 06 July 2022
PUBLISHED 02 September 2022

CITATION
Shi W, Meng Z and Luo J (2022) Connexin 43 (Cx43) regulates high-glucose-induced retinal endothelial cell angiogenesis and retinal neovascularization.
Front. Endocrinol. 13:909207.
doi: 10.3389/fendo.2022.909207

Connexin 43 (Cx43) regulates high-glucose-induced retinal endothelial cell angiogenesis and retinal neovascularization

Wen Shi[1,2], Zhishang Meng[1,2] and Jing Luo[1,2]*

[1]Department of Ophthalmology, The Second Xiangya Hospital, Central South University, Changsha, China, [2]Department of Ophthalmology, Hunan Clinical Research Center of Ophthalmic Disease, Changsha, Hunan, China

Diabetic retinopathy (DR) is an important microvascular complication of type 1 and type 2 diabetes mellitus (DM) and a major cause of blindness. Retinal neovascularization plays a critical role in the proliferative DR. In this study, high glucose-induced connexin 43 (Cx43) expression in human retinal endothelial cells (hRECs) in a dose-dependent manner. Compared with hRECs under normal culture conditions, high-glucose (HG)-stimulated hRECs showed promoted tubule formation, increased ROS release, and elevated levels of tumor necrosis factor-alpha (TNF-α), interleukin-1β (IL-1β), vascular endothelial growth factor A (VEGFA), and intercellular adhesion molecule 1 (ICAM-1) in the culture medium. HG-induced alterations were further magnified after *Cx43* overexpression, whereas partially eliminated after *Cx43* knockdown. Finally, in the DR mouse model, impaired retinal structure, increased CD31 expression, and elevated mRNA levels of *TNF-α*, *IL-1β*, *VEGFA*, and *ICAM-1* were observed; *in-vivo Cx43* knockdown partially reversed these phenomena. Conclusively, *Cx43* knockdown could inhibit hREC angiogenesis, therefore improving DR in the mouse model.

KEYWORDS

diabetic retinopathy, retinal neovascularization, human retinal endothelial cells, angiogenesis, connexin 43 (Cx43)

Introduction

Diabetic retinopathy (DR) is an important microvascular complication of type 1 and type 2 diabetes mellitus (DM), which makes great contributions to blindness (1, 2). Due to the increasing prevalence of DM, DR is increasingly widespread and endangers the vision of patients (3–5). For diabetic tractional retinal detachment in proliferative DR, an advanced form of DR, pars plana vitrectomy is typically performed to repair vision or avoid additional visual loss (6).

The pathology of DR is complex, involving retinal inflammation, increased retinal vascular permeability, and blood-retinal barrier breakdown (7). These malignant processes result in the uncontrolled proliferation and migration of retinal microvascular endothelial cells and the formation of capillary, leading to retinal neovascularization (8). It has been pointed out that retinal neovascularization is one of the most common causes of retinal detachment, vitreous hemorrhage, and sight loss in the proliferative DR (9). Therefore, understanding the underlying mechanisms of retinal neovascularization may provide an effective therapeutic approach for DR. Vascular endothelial growth factor (VEGF) has been proposed as a potent mediator of DR angiogenesis, and VEGF-targeting drugs (such as ranibizumab and aflibercept) have shown promising results (10). Nevertheless, other pro-inflammatory and pro-fibrotic mediators [such as tumor necrosis factor-α (TNF-α), monocyte chemotactic protein 1 (MCP-1), and intercellular adhesion molecule-1 (ICAM-1)] are evidenced to be involved in anti-VEGF therapeutic failure (11). Therefore, more mechanisms of retinal neovascularization through retinal endothelial cells (RECs) in DR must be further validated.

Intercellular communication has been evidenced to contribute greatly to vascular function and homeostasis. Connexins (Cxs) exert crucial effects on this interaction. Cxs, cataloged as transmembrane proteins, form hemichannels in the plasma membrane and intercellular channels, termed gap junctions, connecting the cytoplasm of two adjacent cells (12, 13). As has been reported previously, on vascular walls, 4 Cxs (Cx37, Cx40, Cx43, and Cx45) are found within endothelial cells and smooth muscle cells (12, 13). Endothelial cell proliferation and migration are needed for angiogenesis, finally forming stabilized vessels by recruiting mural cells. Accumulating studies have shown that endothelial Cxs are tightly implicated in modulating these processes (14–17). Knocking out endothelial Cxs reduces angiogenesis (18). On the contrary, upregulated endothelial Cxs (such as Cx37, Cx43, and Cx40) are linked to angiogenesis induction (19, 20). Multiple studies have evidenced that Cx43 is essential for the positive regulation of endothelial cell and endothelial progenitor cell (EPC) migration (21–24). Consistently, Cx43siRNA treatment notably inhibited human late EPC abilities of migration and angiogenesis; within a mouse ischemic hind limb model, the therapeutic angiogenesis capacity of these EPCs is lost (25). Moreover, Cx43 expression is consistent with the increased levels of representative angiogenic factors in rat mesenchymal stem cells with Cx43 overexpression (26). Taken together, the above findings indicated a strong potential of endothelial Cx43 in promoting angiogenesis.

In this study, human RECs (hRECs) were first stimulated with high-glucose (HG) to simulate the DR microenvironment. Cx43 expression was validated in hRECs under normal or HG conditions. hREC tubule formation, reactive oxygen species (ROS) release, and the levels of inflammatory and angiogenesis markers (TNF-α, IL-1β, VEGFA, and ICAM-1) were investigated in normal or HG-treated hRECs. Cx43 overexpression/knockdown was achieved in normal or HG-treated hRECs to explore the *in-vitro* effects of Cx43 overexpression/knockdown on angiogenesis. Finally, the DR mouse model was induced; Cx43 knockdown was achieved through lentivirus infection to evaluate the *in-vivo* effects of Cx43 knockdown on DR angiogenesis. During diabetic retinopathy, high glucose causes endothelial cells to undergo a bidirectional activation of the inflammatory and epigenetic machinery, which eventually results in chronic inflammation and vascular problems, causing globally high morbidity and mortality (27, 28). Therefore, our findings identify *Cx43*siRNA as a druggable target for DR *via* regulating endothelial angiogenesis.

Materials and methods

Cell lineage and cell culture

hRECs (Cat. #6530, ScienCell, Carlsbad, CA, USA) were cultured (37°C, 5% CO_2) in Endothelial Cell Medium (ECM, Cat. #1001, ScienCell) containing 5% fetal bovine serum (FBS; Cat. #0025, ScienCell). hRECs were allocated into four groups: normal, low-HG (culture medium containing 20 mmol/L glucose), middle-HG (culture medium containing 60 mmol/L glucose), and high-HG (culture medium containing 120 mmol/L glucose).

Immunoblotting

Cells were collected using 0.05% Trypsin-EDTA (Thermo Scientific, Waltham, MA, USA). After phosphate-buffered saline (PBS) rinsing, cells were lysed using radioimmunoprecipitation assay (RIPA) buffer (Beyotime, Jiangsu, China). Protein concentration was measured using a BCA Protein Assay kit (Beyotime). Equivalent quantities of protein (30 μg) were injected and then loaded onto 12% sodium dodecyl sulfate-polyacrylamide gel electrophoresis (SDS-PAGE) for separation, followed by the transferring of gels onto polyvinylidene difluoride (PVDF) membranes (Millipore, Billerica, MA). After that, the membranes were blocked in 5% non-fat milk for 1 h at room temperature and then incubated (4°C, overnight) with primary antibodies anti-Cx43 (#3512, Cell Signaling Technology, Danvers, MA, USA) and Tubulin (11224-1-AP, Proteintech, USA). Following 1-h incubation (room temperature) with horseradish-peroxidase (HRP)-conjugated secondary antibodies. Finally, the blots were visualized using Super Enhanced Chemiluminescence (ECL) Detection Reagent (Beyotime), and the signals were analyzed using ImageJ software. Chemiluminescence was determined using a Tanon 5200 Chemiluminescent Imaging System (Tanon, Shanghai, China).

Tubule formation assay

Tube formation assay was performed on Matrigel (BD Biosciences, Franklin Lakes, NJ, USA) to assess angiogenesis. In brief, 10 mg/ml Matrigel (50 μl/well) in serum-free media was applied to 96-well plates, followed by a 30-min incubation at 37°C. HG-stimulated or transfected cells were seeded onto Matrigel-coated plates and then incubated (6 h, 37°C) in the cell culture incubator. Photographs obtained using a light microscope (Olympus, Japan). The tubule formation in each image was quantified using ImageJ software.

Flow cytometry detecting ROS content

ROS production in hRECs was detected using the Reactive Oxygen Species Assay Kit (Beyotime). Specifically, live cells underwent 30-min incubation (37°C) in the serum-free culture medium containing 10 mM 2,7-dichlorofluorescein diacetate (DCFH-DA; Beyotime) or PBS (as blank) in the dark for detecting intracellular ROS level. Next, after trypsinization, the cells were rinsed again in PBS and resuspended (1×10^6 cells/mL) in a serum-free medium for flow cytometry analysis (Novocyte, Agilent, USA). The fsc/ssc scatters were shown in Figure S1.

Enzyme-linked immunosorbent assay

The protein contents of hRECs-released TNF-α, IL-1β, VEGFA, and ICAM-1 in the conditioned medium were determined using corresponding commercially available human ELISA kits (CUSABIO, China). The conditioned medium was harvested and subjected to 15-min centrifugation (350 × g, 4°C) for cellular debris removal. After that, the conditioned medium was recollected and maintained at -80°C for a subsequent ELISA assay.

Cell transfection

The vector containing shRNA for the human *Cx43* gene (sh-Cx43#1/2/3; GenePharma, Shanghai, China) and/or human *Cx43* gene coding sequence (Cx43 OE, GenePharma) were obtained for cell transfection. Cells were transfected after growing to 60% density in culture plates. Next, hRECs were transfected with knockdown/overexpression vector (final concentration 2 μg/ml) using lipo3000 (5 μl/well, Invitrogen, USA). After 48 h, the cells were harvested for the subsequent experiments. The primers for vector sh-CX43#1/2/3 and CX43OE construction were listed in Table 1.

Establishment of DR model of mice

A total of 24 C57BL/6 J mice (6 weeks, 23 ± 2.34 g, male) procured from Changsha SLAC laboratory animal company (Changsha, China) were kept under 12/12 light/dark cycles, with free access to a normal chow diet. All the animal experimental procedures were conducted in compliance with the principles of laboratory animal care (National Institutes of Health, Bethesda, MD, USA) and Use of Animals in Ophthalmic and Vision Research and under the approval of the Second Xiangya Hospital of Central South University (approval number:2018005). Mice were randomly allocated into 4 groups (n=6): normal, DR model, DR + Lv-sh-NC, and DR + Lv-sh-Cx43.

Mice were intraperitoneally injected with 50 mg/kg streptozotocin (STZ) every day for 5 consecutive days for DR model induction. Mice were examined for blood glucose once a week. After STZ injection for 1 to 4 weeks, hyperglycemia occurred; after STZ injection for 16 weeks, mice were sacrificed for tissue collection.

At weeks 4, 8 and 12, and 16 after STZ injection, mice in the DR + Lv-sh-NC and DR + Lv-sh-Cx43 groups were intravitreally injected with sh-NC or sh-Cx43 lentivirus (2×10^6 TU lentivirus in 1 μL, GeneChem, Shanghai, China) in the right eye. Briefly, after mouse eyes were dilated with compound tropicamide, the needle was inserted 1 mm outside the corneal limbus using a microsyringe for intravitreal injection. Mice were anesthetized with isoflurane (3%) in oxygen and underwent intravitreal injection.

Hematoxylin and eosin staining

Mice were sacrificed under anesthesia. The enucleated eyes were fixed overnight in 4% paraformaldehyde at ambient temperature, paraffin-embedded, and then sectioned (5 μm). Next, H&E staining was performed.

Immunofluorescent staining

Tissue samples were fixed in 4% paraformaldehyde, dehydrated with an alcohol gradient, paraffin-embedded, and sectioned. After deparaffinization, the sections were incubated (4°C, overnight) with a primary anti-CD31 antibody (11265-1-AP, Proteintech), and washed 3 times in PBS followed by a 1-h incubation (room temperature) with Cy5-labeled secondary antibody (Beyotime). After PBS washing, the sections underwent 5-min incubation in DAPI (Sigma-Aldrich, USA). Finally, the coverslips were mounted with glycerol, and fluorescence microscopy (Olympus) was applied for analysis.

10.3389/fendo.2022.909207

TABLE 1 The sequence of RT-PCR primer and shRNA.

RT-PCR primer (mouse)	Forward 5'-3'	Reverse 5'-3'
CD31	ACCGGGTGCTGTTCTATAAGG	TCACCTCGTACTCAATCGTGG
TNF-α	CCCTCACACTCAGATCATCTTCT	GCTACGACGTGGGCTACAG
IL-1β	CTGTGACTCATGGGATGATGATG	CGGAGCCTGTAGTGCAGTTG
VEGFA	CGATGAAGCCCTGGAGTGCGT	ACAAACAAATGCTTTCTCCGCTCTG
ICAM-1	GGCATTGTTCTCTAATGTCTCCG	TGTCGAGCTTTGGGATGGTAG
Tubulin	GCATTAACTACCAGCCTCCCAC	CGCCTTCCACAGAATCCACAC
Vector construction primer (human)	Forward 5'-3'	Reverse 5'-3'
Cx43 overexpression	CTACCGGACTCAGATCTCGAGATGGGTGACTGGAGCGCC	GTACCGTCGACTGCAGAATTCCTAGATCTCCAGGTCATCAGGCC
Sh-NC	GATCCGCCAAGCCCTTGTCTTCACAACTCGAGTTGTGAAGACAAGGGCTTGGCTTTTTG	AATTCAAAAAGCCAAGCCCTTGTCTTCACAACTCGAGTTGTGAAGACAAGGGCTTGGCG
Sh-Cx43 1	GATCCGTATTGAAGAGCATGGTAAGGCTCGAGCCTTACCATGCTCTTCAATACTTTTTG	AATTCAAAAAGGATTGAAGAACACGGCAAGGCTCGAGCCTTACCATGCTCTTCAATACG
Sh-Cx43 2	GATCCGGGTCCTGCAGATCATATTTGCTCGAGCAAATATGATCTGCAGGACCCTTTTTG	AATTCAAAAAGGGTCCTGCAGATCATATTTGCTCGAGCAAATATGATCTGCAGGACCCG
Sh-Cx43 3	GATCCGCCACTAGCCATTGTGGACCACTCGAGTGGTCCACAATGGCTAGTGGCTTTTTG	AATTCAAAAAGCCACTAGCCATTGTGGACCACTCGAGTGGTCCACAATGGCTAGTGGCG
Vector construction primer (mouse)	Forward 5'-3'	Reverse 5'-3'
lv-sh-Cx43	GATCCGGGTCCTTCAGATCATATTCGCTCGAGCGAATATGATCTGAAGGACCCTTTTTG	AATTCAAAAAGGGTCCTTCAGATCATATTCGCTCGAGCGAATATGATCTGAAGGACCCG
lv-Sh-NC	GATCCGCCAAGCCCTTGTCTTCACAACTCGAGTTGTGAAGACAAGGGCTTGGCTTTTTG	AATTCAAAAAGCCAAGCCCTTGTCTTCACAACTCGAGTTGTGAAGACAAGGGCTTGGCG

Quantitative reverse transcription-polymerase chain reaction

Total RNA was isolated from target tissues or cultured cells using TRIzol reagent (Invitrogen) as per the manufacturer's instructions. cDNAs were synthesized using the M-MLV Reverse Transcriptase Kit (ELK Biotechnology, Wuhan, China) for mRNA expression assessment. Real-time PCR was performed using a StepOne™ Real-Time PCR instrument (Thermo Scientific). Tubulin served as a loading control to measure the mRNA level, and the $2^{-\Delta\Delta Ct}$ method was used for calculation. The primer sequence was listed in Table 1.

Statistical analysis

All data were expressed as mean ± standard deviation (SD). GraphPad Prism (GraphPad Software, Inc., La Jolla, CA, USA) was employed for data analysis. Two-group comparisons were analyzed using Student's *t*-test; multiple comparisons were analyzed using one-way ANOVA with Tukey's *post-hoc* test. $P<0.05$ was considered statistically significant.

Results

HG impairs human retinal endothelial cell functions

For the minimum HG dose selection, hRECs were stimulated with gradient concentrations of glucose (20, 60, or 120 mmol/L) and examined for Cx43 protein level. As indicated by the results, 60 or 120 mmol/L HG dramatically increased the Cx43 protein level relative to the normal culture medium (Figure 1A). Therefore, 60 mmol/L HG was selected for the subsequent experiments. In the meantime, a mannitol treatment group (60 mmol/L) was set to exclude the osmotic effect. As shown in Figures 1B-D, mannitol treatment caused no significant alterations in cell phenotypes, including tubule formation, ROS release, and the levels of TNF-α, IL-1β, VEGFA, and ICAM-1 in the culture medium compared with the control group. After 60 mmol/L HG stimulation, hREC functions were examined. It was observed that HG stimulation significantly promoted hREC tubule formation (Figure 1B), ROS release (Figure 1C), and TNF-α, IL-1β, VEGFA, and ICAM-1 levels in the culture medium (Figure 1D).

Effects of Cx43 knockdown or overexpression on HG-induced angiogenesis

hRECs were transfected with the vector containing shRNA targeting *Cx43* (sh-Cx43#1/2/3) or *Cx43* coding sequence (Cx43 OE) for *Cx43* knockdown/overexpression to investigate *Cx43*-

10.3389/fendo.2022.909207

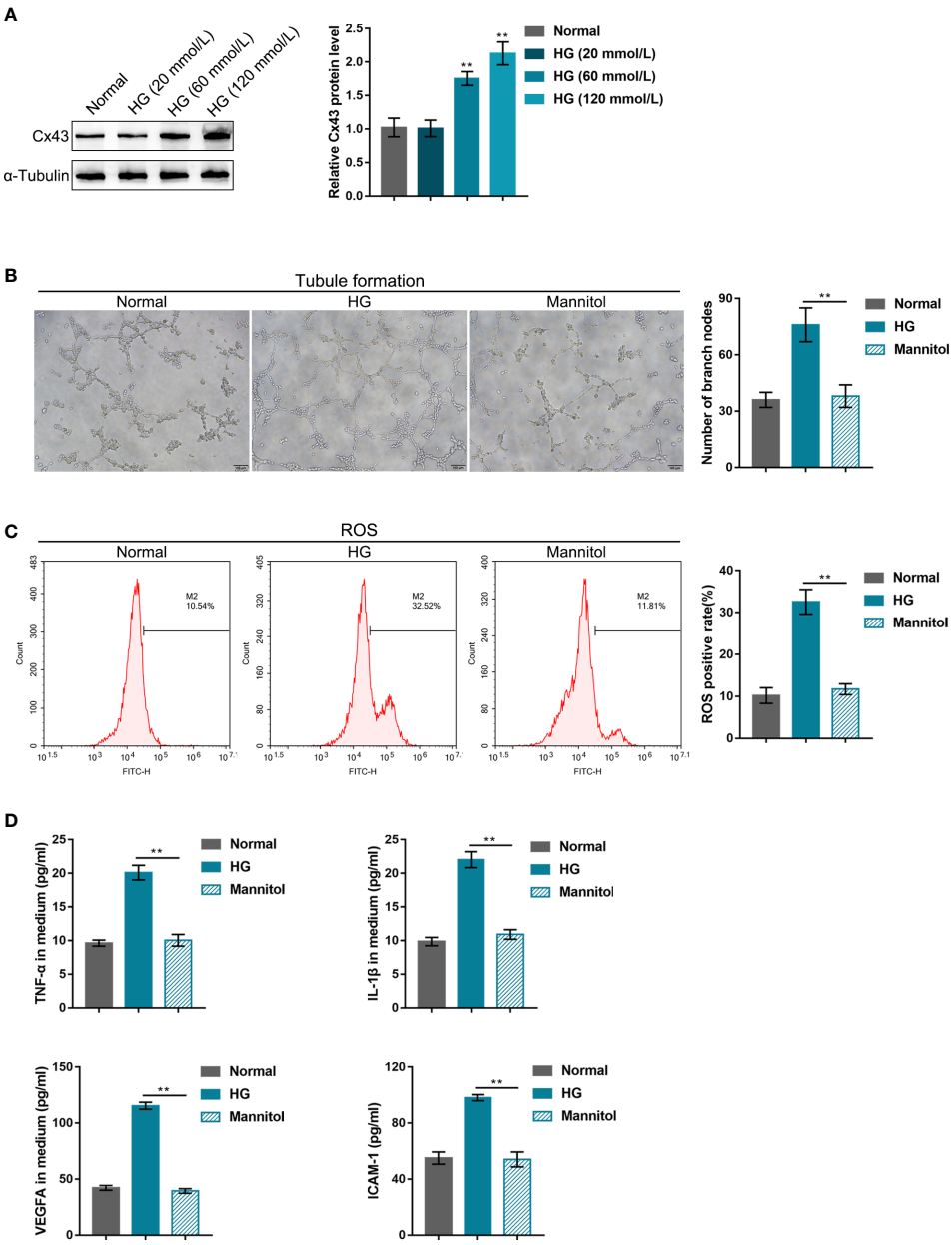

FIGURE 1
High-glucose (HG) impairs human retinal endothelial cell functions **(A)** hRECs were stimulated with gradient concentrations of glucose (20, 60, or 120 mmol/L) and examined for connexin 43 (Cx43) protein level using Immunoblotting. hRECs were subsequently stimulated with HG (60 mmol/L) or mannitol (60 mmol, to exclude the osmotic effect) and examined for tubule formation on Matrigel **(B)**; ROS release using flow cytometry **(C)**; the content of tumor necrosis factor alpha (TNF-α), interleukin-1β (IL-1β), vascular endothelial growth factor A (VEGFA), and intercellular adhesion molecule 1 (ICAM-1) in culture medium using ELISA kits **(D)**. n = 3, **p<0.01 compared with the normal group.

specific effects on HG-induced angiogenesis. *Cx43* knockdown or overexpression was confirmed using Immunoblotting (Figures 2A, 3A), and sh-Cx43#2 was selected for the subsequent experiments. The transfected cells were cultured in the normal or HG medium and examined for angiogenesis. The results revealed that HG stimulation promoted hREC tubule formation (Figures 2B, 3B), elevated hREC ROS release (Figures 2C, 3C), and increased TNF-α, IL-1β, VEGFA, and ICAM-1 levels in the culture medium (Figures 2D, 3D). Under normal culture conditions, *Cx43* knockdown remarkably inhibited hREC tubule formation (Figure 2B), reduced hREC ROS production (Figure 2C), and decreased TNF-α, IL-1β, VEGFA, and ICAM-1 levels in the culture medium (Figure 2D); *Cx43* overexpression caused the opposite effects to *Cx43* knockdown on hREC angiogenesis, as

10.3389/fendo.2022.909207

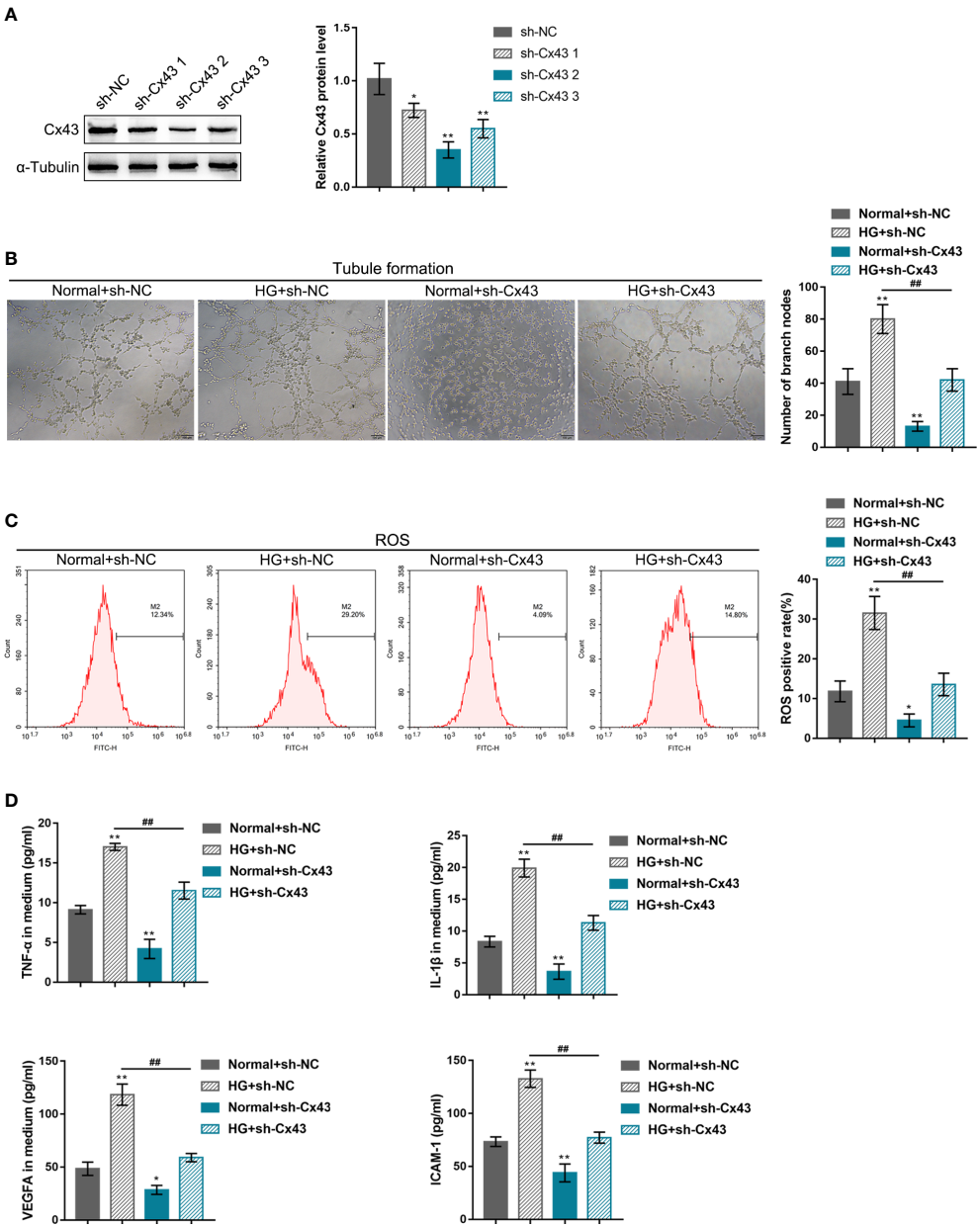

FIGURE 2
Effects of *Cx43* knockdown on HG-induced angiogenesis **(A)** Cx43 knockdown in hRECs was achieved through the transfection of the vector containing small hairpin RNA targeting *Cx43* (sh-Cx43#1/2/3); *Cx43* knockdown was confirmed using Immunoblotting. hRECs were subsequently transfected with sh-Cx43#2 (with better knocking down efficiency), cultured in normal or 60 mmol/L HG medium, and examined for tubule formation on Matrigel **(B)**; ROS release using flow cytometry **(C)**; the content of TNF-α, IL-1β, VEGFA, and ICAM-1 in culture medium using ELISA kits **(D)**. n = 3, *p < 0.05, **p < 0.01 compared with normal+sh-NC group; $^{\#\#}$p < 0.01 compared with HG+sh-NC group.

manifested by the promoted tubule formation (Figure 3B), elevated ROS release (Figure 3C), and increased TNF-α, IL-1β, VEGFA, and ICAM-1 levels in the culture medium (Figure 3D). The promoting effects of HG on hREC angiogenesis were partially eliminated after *Cx43* knockdown (Figures 2B–D), whereas even magnified after *Cx43* overexpression (Figures 3B–D). From all above, *Cx43* knockdown attenuates, whereas *Cx43* overexpression promotes HG-induced hREC angiogenesis. Furthermore, the effects of oxidative stress alone or combined with an antioxidant (N-Acetyl Cysteine, NAC) on hRECs were determined to investigate whether Cx43 could be regulated by ROS. Figure S2 shows that ROS release was dramatically elevated by HG stimulation and partially decreased by NAC treatment (Figure S2A); in the meantime, HG-induced Cx43 protein levels elevation was partially reduced

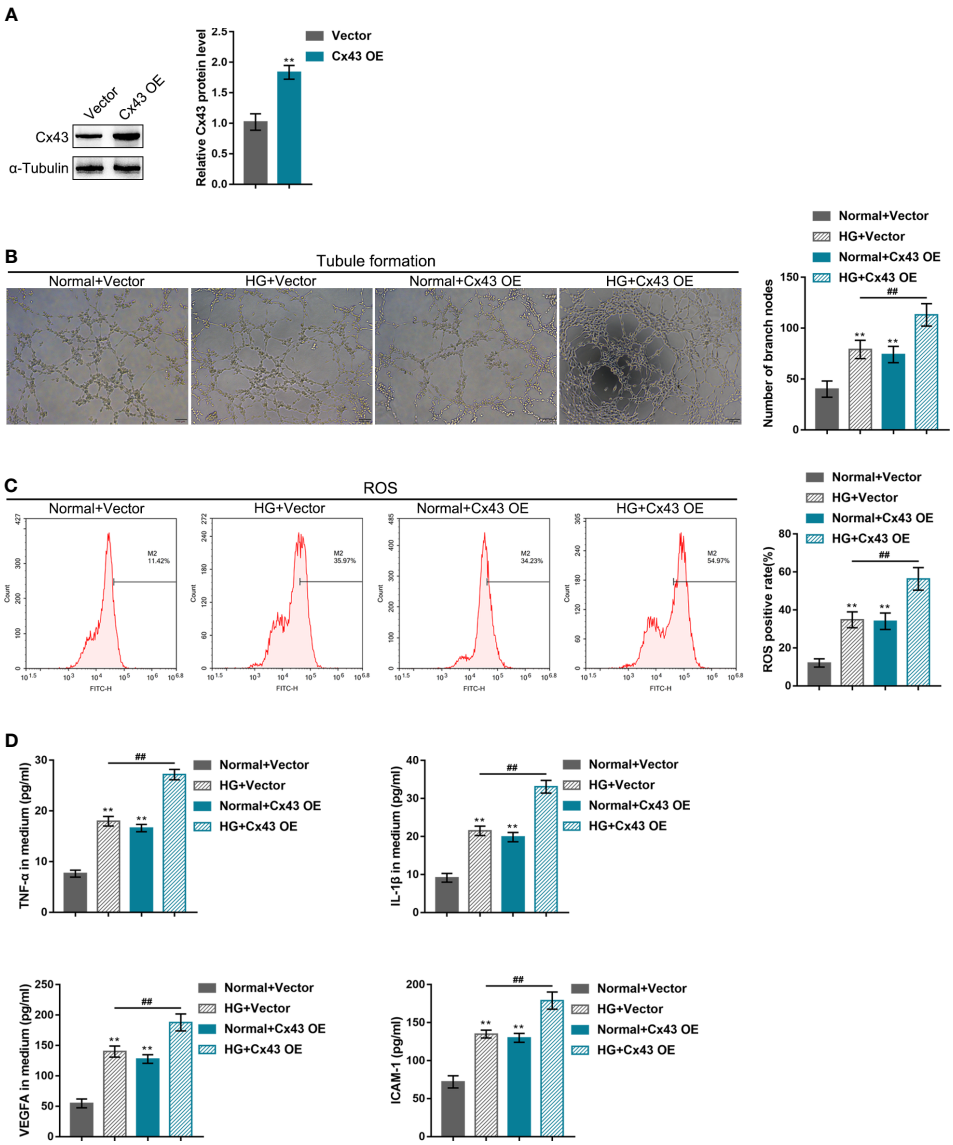

FIGURE 3
Effects of *Cx43* overexpression on HG-induced angiogenesis **(A)** *Cx43* overexpression in hRECs was achieved through transfection of the vector containing *Cx43* gene coding sequence (Cx43 OE); *Cx43* overexpression was confirmed using Immunoblotting. hRECs were subsequently transfected with Cx43 OE, cultured in normal or 60 mmol/L HG medium, and examined for tubule formation on Matrigel **(B)**; ROS release using flow cytometry **(C)**; the content of TNF-α, IL-1β, VEGFA, and ICAM-1 in culture medium using ELISA kits **(D)**. n = 3, $^{**}p < 0.01$ compared with normal+vector group; $^{\#\#}p < 0.01$ compared with HG+vector group.

by NAC treatment (Figure S2B). Therefore, Cx43 might be regulated by ROS.

In-vivo effects of Cx43 knockdown on DR mouse model

The DR mouse model was induced through sh-Cx43 lentivirus infection into C57BL/6 J mice as previously described to investigate the *in-vivo* effects of Cx43 on retinal neovascularization during DR (29). The body weight and blood glucose of mice in each group were monitored; Figures 4A, B shows that mice in the DR and DR + Lv-sh-NC groups saw significantly decreased body weight and elevated blood glucose, whereas intravitreally injection of Lv-sh-Cx43-induced *Cx43* knockdown in retina did not affect mice body weight and reduced blood glucose. As indicated by H&E staining results, the disorder in cell layers reduced thickness of the retina and microvessels in the inner plexiform layer (IPL) were observed in the DR and DR + Lv-sh-NC groups, which were partially

improved after Lv-sh-Cx43 infection (Figure 4C). CD31 levels in the retina (a marker of retinal neovascularization) were examined using IF staining, and its mRNA expression was determined using qRT-PCR. The results revealed that CD31 level was markedly elevated in the DR and DR + Lv-sh-NC groups whereas partially reduced after Lv-sh-Cx43 infection (Figures 4D, E). Cx43 knockdown in the retina was also confirmed using Immunoblotting; Figure 4F shows that the levels of Cx43 were significantly elevated in the DR groups, whereas effectively decreased by Lv-sh-Cx43 infection (Figure 4F). *TNF-α*, *IL-1β*, *VEGFA*, and *ICAM-1* mRNA levels in tissues were detected, which were observed to be remarkably upregulated in the DR and DR + Lv-sh-NC groups whereas partially downregulated after Lv-sh-Cx43 infection (Figure 4G).

Discussion

In this study, high glucose increased *Cx43* expression in hRECs in a dose-dependent manner. Compared with hRECs

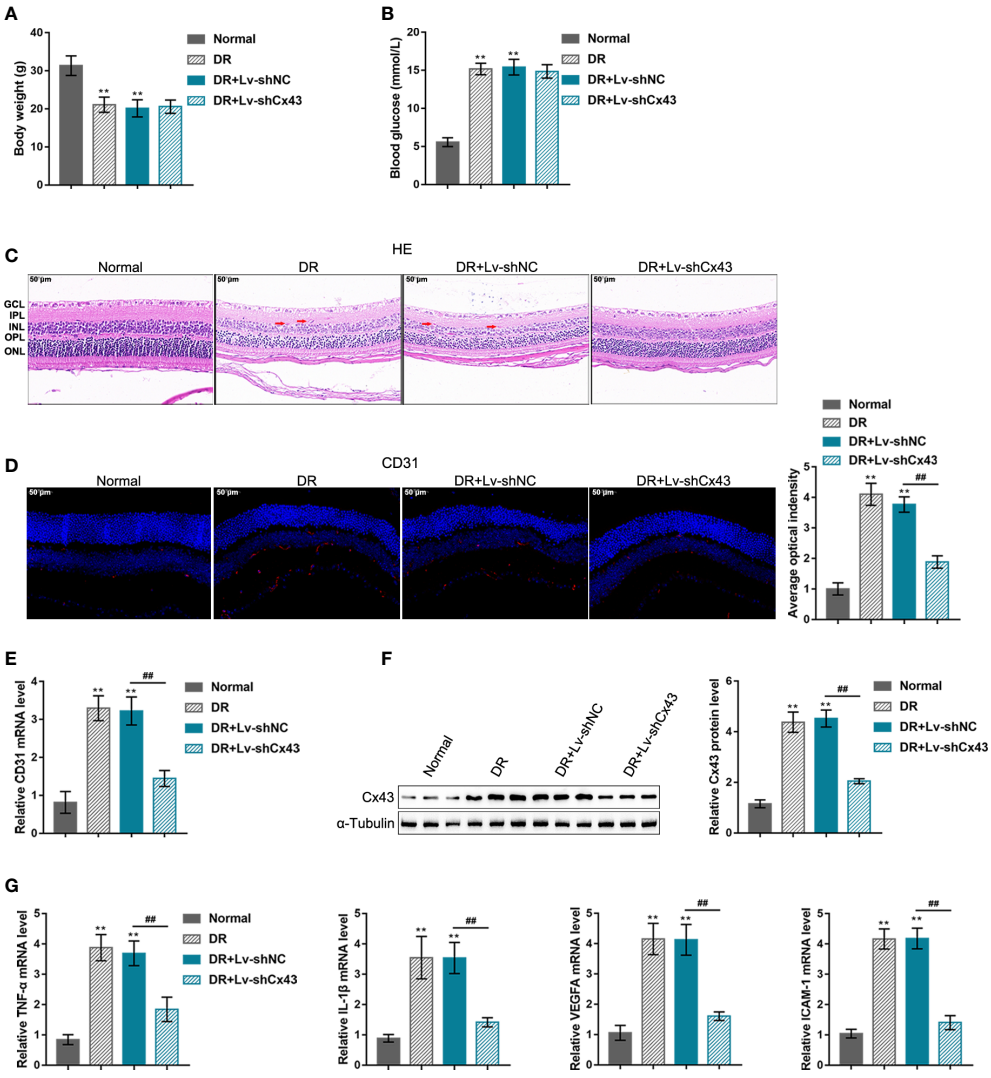

FIGURE 4
in-vivo effects of *Cx43* knockdown on the DR mouse model DR model was induced in C57BL/6 J mice and lentivirus infection as previously described. **(A, B)** Body weight and blood glucose of mice in different groups were determined. **(C)** The histopathological alterations in the retina were examined using H&E staining. ganglion cell layer (GCL); inner plexiform layer (IPL); inner nuclear layer (INL), outer plexiform layer (OPL); outer nuclear layer (ONL). Red arrows indicated microvessels. **(D)** CD31 levels in the retina were examined using IF staining. **(E)** The mRNA expression of CD31 in the retina was determined using qRT-PCR. **(F)** The protein levels of Cx43 in the retina were determined using Immunoblotting. **(G)** The mRNA expressions of TNF-α, IL-1β, VEGFA, and ICAM-1 in tissue samples were examined using qRT-PCR. n = 6, $^{**}p < 0.01$ compared with normal group; $^{\#\#}p < 0.01$ compared with DR+Lv-shNC group.

under normal culture conditions, HG-stimulated hRECs showed notably promoted tubule formation, ROS release, and TNF-α, IL-1β, VEGFA, and ICAM-1 levels in the culture medium. These HG-induced alterations were further magnified after *Cx43* overexpression, whereas partially eliminated after *Cx43* knockdown. Finally, in the DR mouse model, impaired retina structure, increased CD31 level (a marker of retinal neovascularization), and upregulated mRNA levels of TNF-α, IL-1β, VEGFA, and ICAM-1 were observed; *in-vivo Cx43* knockdown partially reversed these phenomena s.

During DR, pathological angiogenesis is one of the leading causes of permanent blindness in people of all ages. One of the key pathological conditions contributing to these vision-threatening retinopathies is retinal neovascularization (30, 31). The term angiogenesis was initially utilized to explain the sprouting of new capillaries from the pre-existing postcapillary venules (32). As aforementioned, angiogenesis is a complex process, in which tubule formation by endothelial cells is a critical event (32, 33). In the present study, HG stimulation increased Cx43 levels in hRECs in a dose-dependent manner, which suggested the potential role of Cx43 in hREC angiogenesis. As expected, HG stimulation dramatically promoted hREC tubule formation, further enhanced after *Cx43* overexpression, whereas partially attenuated after *Cx43* knockdown. Moreover, as evidenced previously, *Cx43* siRNA-treated EPCs lose their therapeutic angiogenic potential in a mouse hindlimb ischemia model (25). Consistently, the findings in this study further evidenced the promotive role of Cx43 in hREC angiogenesis.

It's well-established that excessive ROS produced under various physiological and pathological conditions [such as inflammation (34) and ischemia (35)] may lead to the metabolic imbalance of oxidative stress-generated reactive intermediates and multiple disorders, including DR (36, 37). A previous study has pointed out that hypoxia-inducible factor (HIF)-1α-mediated hypoxic response is tightly linked to hypoxia-induced ROS production (38). Accumulating studies have shown that VEGF and ROS play key roles in vascular pathophysiology (39, 40). VEGF plays an essential role in the disorder, and its interaction with neutralizing molecules represents a significant advancement in diabetes treatment (41). VEGF could promote the proliferation and migration of vascular endothelial cells, and elicit blood vessel permeability. Hypoxia-induced increase of VEGF has emerged as a major driver of neovascularization in DR (42). In this study, HG-treated hRECs presented elevated ROS release and increased VEGFA levels in the culture medium. Similarly, HG-induced increase of ROS and VEGFA levels were both reduced after *Cx43* knockdown, which suggested that *Cx43* knockdown inhibited HG-induced angiogenesis in hRECs.

As a typical characteristic of diabetes, chronic inflammation also occurs in the eyes (43). Elevated levels of IL-1β and TNF-α are tightly implicated in DR (44). Reportedly, pro-inflammatory cytokines result in the breakdown of the blood-retinal barrier in DR through various molecular mechanisms in the retinal vasculature (45, 46). As a result, the reduced expressions of pro-inflammatory cytokines may show vascular advantages in DR. A previous study has pointed out that Cx43 promotes inflammasome activation and the development of renal inflammatory cell damage through intracellular redox regulation (47). Cx43 has been reported to be involved in both cytokine and immunoglobulin secretion in diseased human corneas; Cx43 in macrophages of distinct tissues could partially enhance the secretion of pro-inflammatory cytokines (48). In this study, HG stimulation dramatically elevated IL-1β and TNF-α levels, which were further amplified after *Cx43* overexpression whereas partially reduced after *Cx43* knockdown. The above data indicated that Cx43 knockdown could improve HG-induced retinal inflammation.

Furthermore, the above findings were further evidenced in an STZ-induced DR mouse model. In the DR mouse model, impaired retina structure, increased CD31 level (a marker of retinal neovascularization), and upregulated mRNA expression levels of TNF-α, IL-1β, VEGFA, and the ICAM-1 were partially abolished after *in-vivo* Cx43 knockdown. In summary, Cx43 knockdown could inhibit hREC angiogenesis and inflammation, therefore improving DR symptoms in the DR mouse model.

Concerning the possible mechanism of Cx43 function on angiogenesis and inflammation, endothelial cells in the retina are strongly stimulated by the coexistence of hyperglycemia and hypoxia, increasing *VEGF* expression (49). Cx43 has been reported to regulate the production of HIF-1 to control VEGF-induced angiogenesis (50). The HIF-1α response to hypoxia is associated with hypoxia-induced production of ROS (38), and ROS triggers the induction of VEGF (51–53). Since supplementary experiments indicate that the elevation of Cx43 protein levels was associated with the ROS accumulation, the mechanism of Cx43 regulating pro-inflammatory factors and angiogenesis might be related to the coexistence of hyperglycemia and hypoxia and oxidative stress, which needs further investigations in our future studies.

Data availability statement

The raw data supporting the conclusions of this article will be made available by the authors, without undue reservation.

Ethics statement

The animal study was reviewed and approved by ethic committee of Xiangya Hospital of Central South University.

Author contributions

WS: performed the experiments, wrote manuscript. ZM: Performed the experiments. JL: Supervision, edited manuscript. All authors contributed to the article and approved the submitted version.

Funding

This study was supported by Natural Science Foundation of Hunan Province, China (2021JJ40862) and Natural Science Foundation of Changsha City, China (kq2014249).

Conflict of interest

The authors declare that the research was conducted in the absence of any commercial or financial relationships that could be construed as a potential conflict of interest.

Publisher's note

Supplementary material

The Supplementary Material for this article can be found online at: https://www.frontiersin.org/articles/10.3389/fendo.2022.909207/full#supplementary-material

SUPPLEMENTARY FIGURE 1
Images with the fluorescein signal combined with the fsc/ssc scatter.

SUPPLEMENTARY FIGURE 2
Effects of 60 mmol/L HG and antioxidant (N-Acetyl Cysteine, NAC, 1mmol/L) on ROS release **(A)** and Cx43 expression **(B)** in hRECs.

References

1. Yau JW, Rogers SL, Kawasaki R, Lamoureux EL, Kowalski JW, Bek T, et al. Global prevalence and major risk factors of diabetic retinopathy. *Diabetes Care* (2012) 35(3):556–64. doi: 10.2337/dc11-1909

2. Lee R, Wong TY, Sabanayagam C. Epidemiology of diabetic retinopathy, diabetic macular edema and related vision loss. *Eye Vis (Lond)* (2015) 2:17. doi: 10.1186/s40662-015-0026-2

3. Wang Y, Lin W, Ju J. MicroRNA-409-5p promotes retinal neovascularization in diabetic retinopathy. *Cell Cycle* (2020) 19(11):1314–25. doi: 10.1080/15384101.2020.1749484

4. Stitt AW, Curtis TM, Chen M, Medina RJ, McKay GJ, Jenkins A, et al. The progress in understanding and treatment of diabetic retinopathy. *Prog Retin Eye Res* (2016) 51:156–86. doi: 10.1016/j.preteyeres.2015.08.001

5. Kollias AN, Ulbig MW. Diabetic retinopathy: Early diagnosis and effective treatment. *Dtsch Arztebl Int* (2010) 107(5):75–83; quiz 84. doi: 10.3238/arztebl.2010.0075

6. Tan CS, Chew MC, Lim LW, Sadda SR. Advances in retinal imaging for diabetic retinopathy and diabetic macular edema. *Indian J Ophthalmol* (2016) 64 (1):76–83. doi: 10.4103/0301-4738.178145

7. Rask-Madsen C, King GL. Vascular complications of diabetes: mechanisms of injury and protective factors. *Cell Metab* (2013) 17(1):20–33. doi: 10.1016/j.cmet.2012.11.012

8. Gardner TW, Antonetti DA, Barber AJ, LaNoue KF, Levison SW. Diabetic retinopathy: more than meets the eye. *Surv Ophthalmol* (2002) 47(Suppl 2):S253–62. doi: 10.1016/S0039-6257(02)00387-9

9. Stitt AW, Bhaduri T, McMullen CB, Gardiner TA, Archer DB. Advanced glycation end products induce blood-retinal barrier dysfunction in normoglycemic rats. *Mol Cell Biol Res Commun* (2000) 3(6):380–8. doi: 10.1006/mcbr.2000.0243

10. Ford JA, Elders A, Shyangdan D, Royle P, Waugh N. The relative clinical effectiveness of ranibizumab and bevacizumab in diabetic macular oedema: an indirect comparison in a systematic review. *BMJ* (2012) 345:e5182. doi: 10.1136/bmj.e5182

11. Flyvbjerg A. Diabetic angiopathy, the complement system and the tumor necrosis factor superfamily. *Nat Rev Endocrinol* (2010) 6(2):94–101. doi: 10.1038/nrendo.2009.266

12. Hautefort A, Pfenniger A, Kwak BR. Endothelial connexins in vascular function. *Vasc Biol* (2019) 1(1):H117–24. doi: 10.1530/VB-19-0015

13. Pohl U. Connexins: Key players in the control of vascular plasticity and function. *Physiol Rev* (2020) 100(2):525–72. doi: 10.1152/physrev.00010.2019

14. Fang JS, Coon BG, Gillis N, Chen Z, Qiu J, Chittenden TW, et al. Shear-induced notch-Cx37-p27 axis arrests endothelial cell cycle to enable arterial specification. *Nat Commun* (2017) 8(1):2149. doi: 10.1038/s41467-017-01742-7

15. Hirschi KK, Burt JM, Hirschi KD, Dai C. Gap junction communication mediates transforming growth factor-beta activation and endothelial-induced mural cell differentiation. *Circ Res* (2003) 93(5):429–37. doi: 10.1161/01.RES.0000091259.84556.D5

16. Kameritsch P, Pogoda K, Pohl U. Channel-independent influence of connexin 43 on cell migration. *Biochim Biophys Acta* (2012) 1818(8):1993–2001. doi: 10.1016/j.bbamem.2011.11.016

17. Matsuuchi L, Naus CC. Gap junction proteins on the move: connexins, the cytoskeleton and migration. *Biochim Biophys Acta* (2013) 1828(1):94–108. doi: 10.1016/j.bbamem.2012.05.014

18. Gartner C, Ziegelhoffer B, Kostelka M, Stepan H, Mohr FW, Dhein S. Knock-down of endothelial connexins impairs angiogenesis. *Pharmacol Res* (2012) 65(3):347–57. doi: 10.1016/j.phrs.2011.11.012

19. Dhein S, Gaertner C, Georgieff C, Salameh A, Schlegel F, Mohr FW. Effects of isoprenaline on endothelial connexins and angiogenesis in a human endothelial cell culture system. *Naunyn Schmiedebergs Arch Pharmacol* (2015) 388(1):101–8. doi: 10.1007/s00210-014-1059-0

20. Li Z, Zhang S, Cao L, Li W, Ye YC, Shi ZX, et al. Erratum: Tanshinone IIA and astragaloside IV promote the angiogenesis of mesenchymal stem cell-derived endothelial cell-like cells *via* upregulation of Cx37, Cx40 and Cx43. *Exp Ther Med* (2018) 16(3):2167. doi: 10.3892/etm.2018.6428

21. Arshad M, Conzelmann C, Riaz MA, Noll T, Gunduz D. Inhibition of Cx43 attenuates ERK1/2 activation, enhances the expression of Cav1 and suppresses cell proliferation. *Int J Mol Med* (2018) 42(5):2811–8. doi: 10.3892/ijmm.2018.3828

22. Behrens J, Kameritsch P, Wallner S, Pohl U, Pogoda K. The carboxyl tail of Cx43 augments p38 mediated cell migration in a gap junction-independent manner. *Eur J Cell Biol* (2010) 89(11):828–38. doi: 10.1016/j.ejcb.2010.06.003

23. Kwak BR, Pepper MS, Gros DB, Meda P. Inhibition of endothelial wound repair by dominant negative connexin inhibitors. *Mol Biol Cell* (2001) 12(4):831–45. doi: 10.1091/mbc.12.4.831

24. Pepper MS, Spray DC, Chanson M, Montesano R, Orci L, Meda P. Junctional communication is induced in migrating capillary endothelial cells. *J Cell Biol* (1989) 109(6 Pt 1):3027–38. doi: 10.1083/jcb.109.6.3027

25. Wang HH, Su CH, Wu YJ, Li JY, Tseng YM, Lin YC, et al. Reduction of connexin43 in human endothelial progenitor cells impairs the angiogenic potential. *Angiogenesis* (2013) 16(3):553–60. doi: 10.1007/s10456-013-9335-z

26. Wang DG, Zhang FX, Chen ML, Zhu HJ, Yang B, Cao KJ. Cx43 in mesenchymal stem cells promotes angiogenesis of the infarcted heart independent of gap junctions. *Mol Med Rep* (2014) 9(4):1095–102. doi: 10.3892/mmr.2014.1923

27. Nensat C, Songjang W, Tohtong R, Suthiphongchai T, Phimsen S, Rattanasinganchan P, et al. Porcine placenta extract improves high-glucose-induced angiogenesis impairment. *BMC Complement Med Ther* (2021) 21(1):66. doi: 10.1186/s12906-021-03243-z

28. Dhawan P, Vasishta S, Balakrishnan A, Joshi MB. Mechanistic insights into glucose induced vascular epigenetic reprogramming in type 2 diabetes. *Life Sci* (2022) 298:120490. doi: 10.1016/j.lfs.2022.120490

29. Thomas AA, Biswas S, Feng B, Chen S, Gonder J, Chakrabarti S. lncRNA H19 prevents endothelial-mesenchymal transition in diabetic retinopathy. *Diabetologia* (2019) 62(3):517–30. doi: 10.1007/s00125-018-4797-6

30. Penn JS, Madan A, Caldwell RB, Bartoli M, Caldwell RW, Hartnett ME. Vascular endothelial growth factor in eye disease. *Prog Retin Eye Res* (2008) 27 (4):331–71. doi: 10.1016/j.preteyeres.2008.05.001

31. Rama N, Dubrac A, Mathivet T, Ni Charthaigh RA, Genet G, Cristofaro B, et al. Slit2 signaling through Robo1 and Robo2 is required for retinal neovascularization. *Nat Med* (2015) 21(5):483–91. doi: 10.1038/nm.3849

32. Carmeliet P. Mechanisms of angiogenesis and arteriogenesis. *Nat Med* (2000) 6(4):389–95. doi: 10.1038/74651

33. Kruger-Genge A, Blocki A, Franke RP, Jung F. Vascular endothelial cell biology: An update. *Int J Mol Sci* (2019) 20(18). doi: 10.3390/ijms20184411

34. Blaser H, Dostert C, Mak TW, Brenner D, Tnf ROS. TNF and ROS crosstalk in inflammation. *Trends Cell Biol* (2016) 26(4):249–61. doi: 10.1016/j.tcb.2015.12.002

35. Redza-Dutordoir M, Averill-Bates DA. Activation of apoptosis signalling pathways by reactive oxygen species. *Biochim Biophys Acta* (2016) 1863(12):2977–92. doi: 10.1016/j.bbamcr.2016.09.012

36. Kang Q, Yang C. Oxidative stress and diabetic retinopathy: Molecular mechanisms, pathogenetic role and therapeutic implications. *Redox Biol* (2020) 37:101799. doi: 10.1016/j.redox.2020.101799

37. Giacco F, Brownlee M. Oxidative stress and diabetic complications. *Circ Res* (2010) 107(9):1058–70. doi: 10.1161/CIRCRESAHA.110.223545

38. Chandel NS, Maltepe E, Goldwasser E, Mathieu CE, Simon MC, Schumacker PT. Mitochondrial reactive oxygen species trigger hypoxia-induced transcription. *Proc Natl Acad Sci U.S.A.* (1998) 95(20):11715–20. doi: 10.1073/pnas.95.20.11715

39. Pearlstein DP, Ali MH, Mungai PT, Hynes KL, Gewertz BL, Schumacker PT. Role of mitochondrial oxidant generation in endothelial cell responses to hypoxia. *Arterioscler Thromb Vasc Biol* (2002) 22(4):566–73. doi: 10.1161/01.ATV.0000012262.76205.6A

40. Maraldi T, Prata C, Caliceti C, Vieceli Dalla Sega F, Zambonin L, Fiorentini D, et al. VEGF-induced ROS generation from NAD(P)H oxidases protects human leukemic cells from apoptosis. *Int J Oncol* (2010) 36(6):1581–9. doi: 10.3892/ijo_00000645

41. Nicholson BP, Schachat AP. A review of clinical trials of anti-VEGF agents for diabetic retinopathy. *Graefes Arch Clin Exp Ophthalmol* (2010) 248(7):915–30. doi: 10.1007/s00417-010-1315-z

42. Sheikpranbabu S, Kalishwaralal K, Venkataraman D, Eom SH, Park J, Gurunathan S. Silver nanoparticles inhibit VEGF-and IL-1beta-induced vascular permeability *via* src dependent pathway in porcine retinal endothelial cells. *J Nanobiotechnol* (2009) 7:8. doi: 10.1186/1477-3155-7-8

43. Al-Kharashi AS. Role of oxidative stress, inflammation, hypoxia and angiogenesis in the development of diabetic retinopathy. *Saudi J Ophthalmol* (2018) 32(4):318–23. doi: 10.1016/j.sjopt.2018.05.002

44. Guarda G, Dostert C, Staehli F, Cabalzar K, Castillo R, Tardivel A, et al. T Cells dampen innate immune responses through inhibition of NLRP1 and NLRP3 inflammasomes. *Nature* (2009) 460(7252):269–73. doi: 10.1038/nature08100

45. Davis BK, Wen H, Ting JP. The inflammasome NLRs in immunity, inflammation, and associated diseases. *Annu Rev Immunol* (2011) 29:707–35. doi: 10.1146/annurev-immunol-031210-101405

46. Liu S, Li Q, Zhang MT, Mao-Ying QL, Hu LY, Wu GC, et al. Curcumin ameliorates neuropathic pain by down-regulating spinal IL-1beta *via* suppressing astroglial NALP1 inflammasome and JAK2-STAT3 signalling. *Sci Rep* (2016) 6:28956. doi: 10.1038/srep28956

47. Huang Y, Mao Z, Zhang Z, Obata F, Yang X, Zhang X, et al. Connexin43 contributes to inflammasome activation and lipopolysaccharide-initiated acute renal injury *via* modulation of intracellular oxidative status. *Antioxid Redox Signal* (2019) 31(16):1194–212. doi: 10.1089/ars.2018.7636

48. Zhai J, Wang Q, Tao L. Connexin expression patterns in diseased human corneas. *Exp Ther Med* (2014) 7(4):791–8. doi: 10.3892/etm.2014.1530

49. Diaz-Coranguez M, Ramos C, Antonetti DA. The inner blood-retinal barrier: Cellular basis and development. *Vision Res* (2017) 139:123–37. doi: 10.1016/j.visres.2017.05.009

50. Yu W, Jin H, Sun W, Nan D, Deng J, Jia J, et al. Connexin43 promotes angiogenesis through activating the HIF-1alpha/VEGF signaling pathway under chronic cerebral hypoperfusion. *J Cereb Blood Flow Metab* (2021) 41(10):2656–75. doi: 10.1177/0271678X211010354

51. Ushio-Fukai M. VEGF signaling through NADPH oxidase-derived ROS. *Antioxid Redox Signal* (2007) 9(6):731–9. doi: 10.1089/ars.2007.1556

52. Jing Y, Liu LZ, Jiang Y, Zhu Y, Guo NL, Barnett J, et al. Cadmium increases HIF-1 and VEGF expression through ROS, ERK, and AKT signaling pathways and induces malignant transformation of human bronchial epithelial cells. *Toxicol Sci* (2012) 125(1):10–9. doi: 10.1093/toxsci/kfr256

53. Chen S, Zhou Y, Zhou L, Guan Y, Zhang Y, Han X. Anti-neovascularization effects of DMBT in age-related macular degeneration by inhibition of VEGF secretion through ROS-dependent signaling pathway. *Mol Cell Biochem* (2018) 448 (1-2):225–35. doi: 10.1007/s11010-018-3328-6